



INSTITUTE FOR DEFENSE ANALYSES

**Lethal Debris Creation Following
Catastrophic and Sub-catastrophic
Untracked Orbital Debris Impacts on
Smallsats**

Daniel L Pechkis, Project Leader

Peter M Mancini
James F Heagy
Robert F Stellingwerf
Joel E Williamsen

OED Final

April 2024

Distribution Statement A. Approved
for public release: distribution is
unlimited.

IDA Product 3001416

INSTITUTE FOR DEFENSE ANALYSES
730 East Glebe Road
Alexandria, Virginia 22305



The Institute for Defense Analyses is a nonprofit corporation that operates three Federally Funded Research and Development Centers. Its mission is to answer the most challenging U.S. security and science policy questions with objective analysis, leveraging extraordinary scientific, technical, and analytic expertise.

About This Publication

This work was conducted by the Institute for Defense Analyses (IDA) under contract HQ0034-19-D-0001, 229982, "Space Domain Awareness," for the Office of the Director, Operational Test and Evaluation. The views, opinions, and findings should not be construed as representing the official position of either the Department of Defense or the sponsoring organization.

Acknowledgments

The IDA Technical Review Committee was chaired by Dr. Heather M. Wojton and consisted of Dr. Courtney A. Au-Yeung, Dr. Rebeca S. Rodriguez, Dr. Jason Sheldon, from the Operational Evaluation Division, and Dr. Cameron J Liang from the Science, Systems and Sustainment Division.

For more information:

Dr. Daniel L Pechkis, Project Leader
dpechkis@ida.org • 703/845-2597

Dr. Heather M. Wojton, Director, Operational Evaluation Division
hwojton@ida.org • (703) 845-6811

Copyright Notice

© 2024 Institute for Defense Analyses
730 East Glebe Road, Alexandria, Virginia 22305 • (703) 845-2000

This material may be reproduced by or for the U.S. Government pursuant to the copyright license under the clause at DFARS 252.227-7013 [Feb. 2014].

Rigorous Analysis | Trusted Expertise | Service to the Nation

INSTITUTE FOR DEFENSE ANALYSES

IDA Product 3001416

**Lethal Debris Creation Following Catastrophic and
Sub-catastrophic Untracked Orbital Debris Impacts
on Smallsats**

Daniel L Pechkis, Project Leader

Peter M Mancini
James F Heagy
Robert F Stellingwerf
Joel E Williamsen

LETHAL DEBRIS CREATION FOLLOWING CATASTROPHIC AND SUB-CATASTROPHIC UNTRACKED ORBITAL DEBRIS IMPACTS ON SMALLSATS

Peter Mancini^{1,*}, Joel Williamsen¹, James Heagy¹, Bob Stellingwerf²

¹ Institute for Defense Analyses, 730 East Glebe Rd, Alexandria, VA 22305, pmancini@ida.org

² Stellingwerf Associates, 11033 Mathis Mtn Drive, Huntsville, AL 35803, rfs@swcp

ABSTRACT

In this study, we use smooth particle hydrodynamics modeling to examine the creation of mission-lethal non-trackable debris from impacts of 10 g, 100 g, and 10 kg spherical and cylindrical objects on small satellite bus structures at 0, 15, 45, and 75 degrees obliquity. Our simulations include impacts at velocities below, approaching, and above the energy-density threshold that typically disables satellite functionality and creates additional lethal debris. We compare the mass distributions resulting from smooth particle hydrodynamics simulations to the distributions derived from NASA's satellite breakup model; NASA's approximation of debris generation aligns well with our simulation results for large, trackable masses but deviates from simulation results for small, non-trackable masses. Results also show only minor differences in satellite damage and debris generation between spherical and cylindrical 10 kg impactors.

Keywords: Smooth particle hydrodynamics code, orbital debris, lethal non-trackable debris

NOMENCLATURE

d	impactor diameter, cm
KE	kinetic energy, J (Joules)
m_i	mass of impactor, mg
m_t	mass of target, mg
ρ	density, kg/cm³
θ_i	impact angle, ° (degrees)
v_i	impact velocity, km/s

1. INTRODUCTION

As the existing orbital environment becomes denser with both new spacecraft and additional debris, understanding the deleterious effects of collisions and other breakup events is critical to maintaining a safe orbital environment. The National Science and Technology Council stated in 2021 that “lethal non-

trackable debris represents the largest quantity of orbital debris of concern and poses significant risk” to satellites in low earth orbit [1]. “Lethal non-trackable” debris is broadly defined as ranging in size from 0.1 to 3 cm. Novel developments in on-orbit optical detection and advancements in ground systems will help reduce the threshold of what is considered “non-trackable” [2, 3]. Presently, however, observations and measurements of on-orbit debris must be collected with ground-based sensors, which can resolve sizes down to roughly 10 cm.

Predicting debris generation from impactor sizes below detectable levels depends on empirical modeling supported by multiple data sources. This paper provides numerical simulation data for those models. The NASA breakup model is one such empirical model. It is heavily used in the orbital debris community to describe the number and size of trackable and non-trackable debris created from on-orbit collisions and explosions [4]. NASA developed the model using both ground-based observations of on-orbit breakup events and laboratory testing, such as the Satellite Orbital Debris Characterization Impact Test (SOCIT).

Since debris-generating (i.e., catastrophic) on-orbit collisions are neither frequent (fortunately) nor instrumented for data collection (unfortunately), most recent hypervelocity impact data have come from laboratory testing (e.g., gas gun shots) [5, 6, 7] or modeling and simulation with numerical hydrocodes [8]. However, few comprehensive datasets exist, as conducting gas gun testing and running spatially and temporally resolved hydrocode simulations both take considerable effort.

This paper implements a smooth particle hydrocode to improve our understanding of satellite breakup caused by impacts with small (lethal non-trackable) debris and large orbital objects and to compare the resulting mass distributions of debris with the NASA breakup model's predictions. We present the size and velocity distributions of debris generated from impacts with

* Corresponding author: pmancini@ida.org

mission-lethal debris that is below and well above the NASA-defined threshold for catastrophic collisions.

2. MATERIALS AND METHODS

Our goal in this study was to provide high-fidelity simulation results for comparison with NASA model results and with recent laboratory data, as well as to obtain additional insights into the breakup physics of a variety of impact kinematics. The output data of interest for this study are the mass, size, and velocity distributions of generated debris.

We compared our results to results from the NASA breakup model as implemented in EVOLVE 4.0 [4]. This breakup model describes the number of fragments of a given size that are created following a satellite breakup event. NASA has determined that a collision will be catastrophic if the relative kinetic energy of the smaller object in an impact divided by the mass of the larger object is equal to or greater than 40 J/g. In other words, the model predicts that catastrophic collisions will occur when

$$\frac{0.5m_i v_i^2}{m_t} > 40 \text{ J/g}, \quad (1)$$

where m_i is the mass of the impactor and m_t is the mass of the target [4]. Assuming the impact meets the criteria for “catastrophic,” the distribution of debris results in the following power law:

$$N(> L_C) = 0.1 (m_t + m_i)^{0.75} L_C^{-1.71}, \quad (2)$$

where $N(> L_C)$ is the number of particles greater than a given L_C , L_C is a characteristic length of the debris fragment (in meters), and $(m_t + m_i)$ is the total mass of the target and impactor (in kg). This study compared the number of fragments predicted in Equation 2 to the results from simulated collisions of a notional satellite bus with objects ranging from below the 40 J/g catastrophic threshold to well above this threshold.

Plotting the predicted number of debris particles on the basis of their mass distribution (instead of their length distribution) required that we convert L_C -based ejecta into mass. In this paper, we used the SOCIT mass prediction equation (see Figure 4-3 in reference [9]). The conversion of L_C to mass is shown in Equation 3:

$$M = 0.0000192 L_C^{2.28}, \quad (3)$$

where M is the predicted mass of the produced fragment (in kg) and L_C is the characteristic length (in cm). The NASA breakup model combines Equations 2 and 3 to predict the cumulative number of particles per fragment length and mass.

Recent lab-based hypervelocity experiments have contributed to the growing library of satellite breakup measurements [5, 6], building upon the foundational SOCIT testing [10, 11] and manually counting and characterizing thousands of fragments. In this study, we also compared our numerical results to these recent experimental contributions.

Figure 1 shows the collision target in this study, a 110 kg 1 m^3 aluminum notional satellite bus that approximately resembles the OneWeb bus (200 kg and $1 \times 1 \times 1.3 \text{ m}$). Our representative satellite contains internal compartments constructed of thin aluminum, batteries, and a hydrazine tank to emulate realistic internal bus components. Because the impactor only impacts the satellite bus, we decided to remove the pair of solar arrays, weighing a total of approximately 30 kg, to save computational resources and reduce simulation run time. However, in reality the solar arrays would contribute to the fragment distribution.

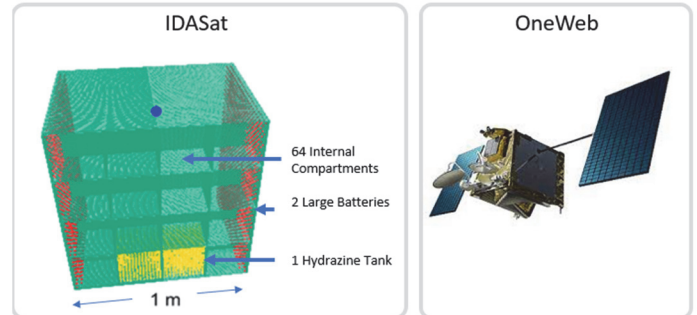


FIGURE 1: (LEFT) MODEL OF THE TARGET SATELLITE BUS WITH 100 g ALUMINUM IMPACTOR AND (RIGHT) A ONEWEB SATELLITE BUS.

This study involved two classes of mission-lethal impactor: lethal non-trackable objects and catastrophically large trackable objects. The former correspond to debris in the 1 to 5 cm range that exist in low earth orbit and can be expected to impact a satellite at orbital velocities relative to the speed of the spacecraft (5 to 10 km/s). The large 10 kg impactor cases represent scenarios that far exceed the 40 J/g threshold and cannot be tested in lab-based experiments. Lethal non-trackable debris objects have been shown to cause the loss of some exposed satellite elements and internal components, such as batteries and radiators [12]. We selected velocity, v , and impact angle, θ_i , for the lethal non-trackable debris cases based on our previous work using ORDEM 3.2 flux predictions at 550 km altitude [13]. Table 1 contains the run matrix for all numerical simulations presented in this study.

Table 1: RUN MATRIX FOR 10 g, 100 g, AND 10 kg ALUMINUM IMPACTORS AGAINST A 110 kg SATELLITE BUS.

	Impactor	$\theta, ^\circ$	m_i, g	d, cm	$v, \text{km/s}$	$KE/m_i, \text{J/g}$
Lethal non-trackable	Aluminum sphere	15, 45, 75	10	1.9	15	6.3
					11	3.4
	100	15	62.5			
		11	33.6			
Catastrophic large object	Aluminum sphere	0	10,000	19, 30, 100	15	5921
					7.5	1480
	Aluminum cylinder	0	10,000	19, 30, 100	4	421

All of the impactor and velocity combinations in Table 1 penetrated the satellite bus and created additional mission-lethal debris. In previous work, we have divided the category of mission-lethal orbital debris into two sub-categories: marginally lethal debris and catastrophically lethal debris [13]. At the lower end of impact energy, marginally lethal debris can disable satellite operations (especially when the debris impacts the satellite’s coolant and electrical lines), whereas catastrophically lethal debris will both disable the satellite and generate vastly more mission-lethal debris following the impact. In both cases, the original impactor may still be small enough to go untracked by most low earth orbit surveillance methods.

For the 10 kg impactors, we chose to hold the mass constant and vary only the shape of the impactor (sphere, cylinder) and cross-sectional impact area. Thus, each of the three 10 kg spheres has a corresponding cylinder with the same diameter and cross-sectional area. We used hollow spheres with variably thick inner walls to increase sphere diameter while holding mass constant. Figure 2 illustrates the six 10 kg impactors used in this study.

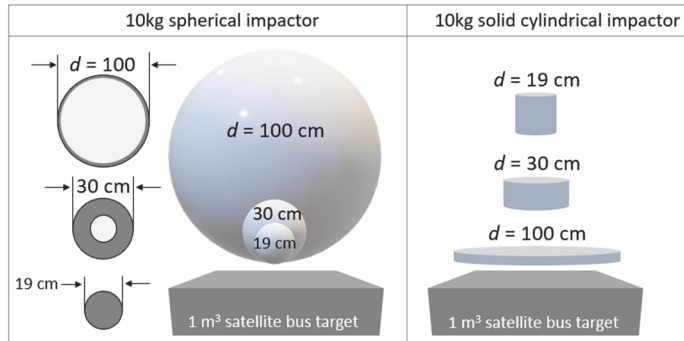


FIGURE 2: SCHEMATICS OF THE SOLID AND HOLLOW SPHERES (LEFT) AND SOLID CYLINDERS (RIGHT) USED AS IMPACTORS.

We used the Smooth Particle Hydrodynamics Code (SPHC) to numerically model hypervelocity impacts [14]. SPHC uses a mesh-free Lagrangian method to accurately model large material deformations and multi-phase interactions. Virtual particles—as opposed to grid vertices—act as interpolation points, and each particle carries material and kinematic information.

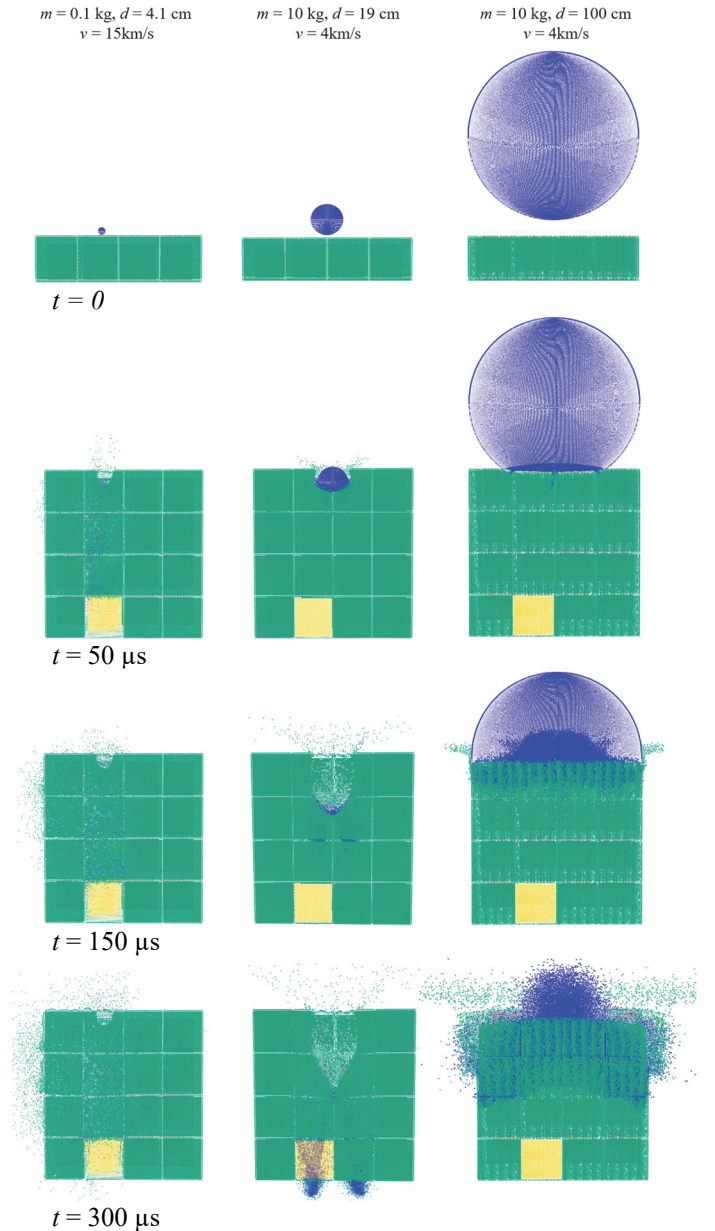
By means of a clustering algorithm, SPHC combines virtual particles into “clusters” that represent material objects, such as the satellite bus or small debris fragments. The output from SPHC provides the properties (m , ρ , L_C), position (x , y , z), and velocity (v_x , v_y , v_z) for each virtual particle and cluster in the simulation.

3. RESULTS AND DISCUSSION

In this section, we present quantitative and qualitative results from the hydrocode runs listed in Table 1 and compare them to existing models and related studies. Then, we describe the cumulative number of generated debris as functions of characteristic length and mass.

3.1 Satellite breakup and debris properties

To provide visual context for the size of the impactor, its penetration depth, and its breakup mechanics, Figure 3 presents a time series of three cases: (left) 100 g solid sphere at 15 km/s, (middle) 10 kg solid sphere at 4 km/s, and (right) 10 kg hollow sphere at 4 km/s. Recall that the lethal non-trackable debris cases hit the target at non-zero impact angles, whereas the large catastrophic impactor cases impacted at 0-degree obliquity for simplicity and because there are no predictions for such large debris objects.



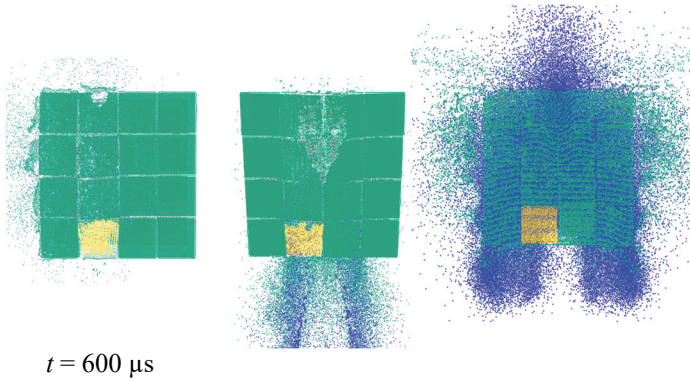


FIGURE 3: HYDROCODE RESULTS FROM THREE HYPERVELOCITY IMPACTS ABOVE THE 40 J/g NASA LIMIT FOR CATASTROPHIC IMPACTS: (LEFT) 100 g SOLID SPHERE, (MIDDLE) 10 kg SOLID SPHERE, AND (RIGHT) 10 kg HOLLOW SPHERE.

As shown in the leftmost column of Figure 3, the 100 g impactor penetrated the satellite bus and created a crater in the topmost bus compartment within the first 50 μs of impact. As expected in hypervelocity impact scenarios and indicated in our simulation data, pressure waves propagated through the satellite bus and there was a rapid phase change of material near the impact location. Additionally, pressure waves traveling through the bus material resulted in spallation on the bottom surface and downward ejecta. Both bus and impactor material were ejected from the top, side, and bottom of the target. Because SPHC provides both the location and the velocity of all fragments in the simulation, we can study both the quantity and the shape of fragments as well as the velocity at which fragments are ejected.

The middle and rightmost columns of Figure 3 present results from two 10 kg cases, a 19 cm solid sphere and a 100 cm hollow sphere. The impact energies per unit mass of the two objects were 421 J/g, an order of magnitude larger than NASA's definition for catastrophic collisions. In both cases, the impactor completely penetrated the entire satellite bus, as illustrated by the blue impactor material exiting the bottom of the bus at $t = 300 \mu\text{s}$ and $600 \mu\text{s}$. The impact of the 19 cm solid sphere formed a cavity slightly wider than its diameter, as predicted by hypervelocity cavity models [15], and a large portion of impactor mass continued through the bus and ejected out the bottom surface. The large hollow sphere, however, impinged the target with a cross-sectional area covering almost the entire target face and penetrated the entire volume of the bus.

Satellite breakup prediction models require information about the quantity, mass, and shape of debris created from a breakup event. Figure 4 presents the distribution of fragment mass as a function of characteristic fragment length for each simulated collision in this study. The figure also plots the fit line from the SOCIT experiment for comparison.

Most notable from the results in Figure 4 is how similar the fragment mass distribution was to the characteristic length distribution both within each impactor mass category and between mass categories. Though the amount of generated debris

differed vastly between impactor masses and shapes, as shown in Figure 3 and discussed further in section 3.2, the trend of generated mass fragments to length of fragment remained consistent.

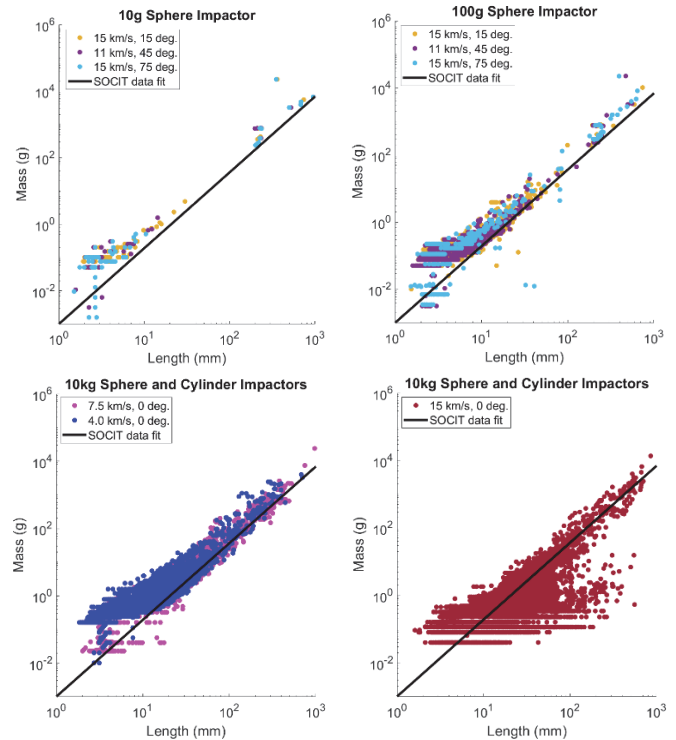


FIGURE 4: FRAGMENT MASS VS. CHARACTERISTIC LENGTH. LETHAL NON-TRACKABLE DEBRIS FOR 10 g IMPACTOR CASE (TOP LEFT) AND 100 g IMPACTOR CASE (TOP RIGHT). LARGE CATASTROPHIC IMPACTORS FOR ALL 4 km/s AND 7.5 km/s CASES (BOTTOM LEFT) AND ALL 15 km/s CASES (BOTTOM RIGHT), INCLUDING 19 cm, 30 cm, AND 100 cm DIAMETER IMPACTORS.

Further, the SOCIT measurement fit line appears to align with the slope of the results from each hydrocode run in this study regardless of impactor mass, shape, or velocity. This finding is consistent with recent lab-based hypervelocity tests, ranging in speed from 2.7 km/s [7] to 7.0 km/s [6]. Murray et al. noted for their hypervelocity impact experiments against the DebrisSat model that “the slope begins to deviate at just under 1 cm and has a distinctly different slope by 1 mm,” [6] which is consistent with the results in Figure 4. In agreement with DebrisSat findings, the SOCIT line generally underpredicts masses for materials with densities ranging from $\rho = 2 \text{ g/cm}^3$ to $\rho = 6 \text{ g/cm}^3$. All material in this study was aluminum with $\rho = 2.71 \text{ g/cm}^3$.

It is also interesting to note that impactor shape (i.e., sphere vs. cylinder) had a negligible effect on the mass-to-length distributions for the 10 kg impactors, as shown in the bottom of Figure 4. The main variable contributing to change in the distribution was impact velocity, but even at different velocities the slope remained consistent.

3.2 Cumulative distributions in mass and length

Figure 5 presents the results for the sum of debris of sizes L_c or larger for all cases in Table 1. In contrast to the general agreement in Figure 4 of results with the NASA mass-to-length model, the results in Figure 5 show much larger deviations from the NASA model in Equation 2. Recall that all 10 g impactor cases in this study fell well below the 40 J/g catastrophic limit that is an inherent assumption within Equation 2. The NASA model predicted several orders of magnitude more debris would be generated than the present hydrocode runs produced. The 100 g cases showed similar results, despite the 15 km/s case exceeding the 40 J/g threshold. The 10 kg sphere and cylinder cases, shown in the bottom row of Figure 5, aligned more closely with the NASA model, though deviations exist and the NASA model generally overpredicted debris relative to SPHC.

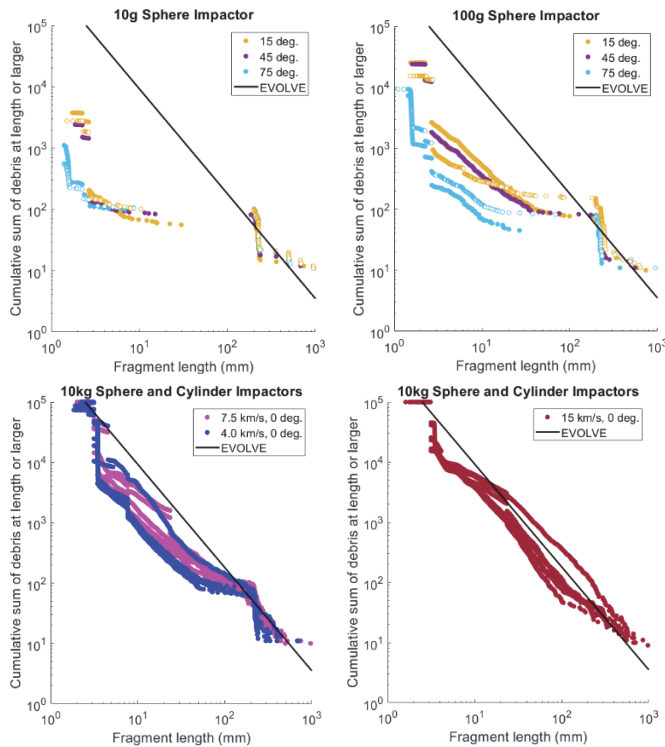


FIGURE 5: CUMULATIVE SUM OF DEBRIS OF SIZES L_c OR LARGER. (TOP) LETHAL NON-TRACKABLE DEBRIS FOR THE 10 g IMPACTOR CASE (LEFT SIDE) AND THE 100 g IMPACTOR CASE (RIGHT SIDE). HOLLOW CIRCLES INDICATE $v = 4$ km/s. (BOTTOM) LARGE CATASTROPHIC IMPACTORS FOR ALL 4 km/s AND 7.5 km/s CASES (LEFT SIDE) AND ALL 15 km/s CASES (RIGHT SIDE), INCLUDING 19 cm, 30 cm, AND 100 cm DIAMETER IMPACTORS.

Figure 6 plots the cumulative sum of debris of masses M or larger. Generally, agreement with the NASA model is similar to that in Figure 5, where the model predicted more debris at each mass than SPHC. However, hydrocode results showed that similar trends exist for runs at a constant impact angle regardless of impact velocity (see 15 degree and 75 degree runs for 10 g and

100 g impactors). The 10 kg impactor cases again aligned more closely with the NASA model for all mass regimes.

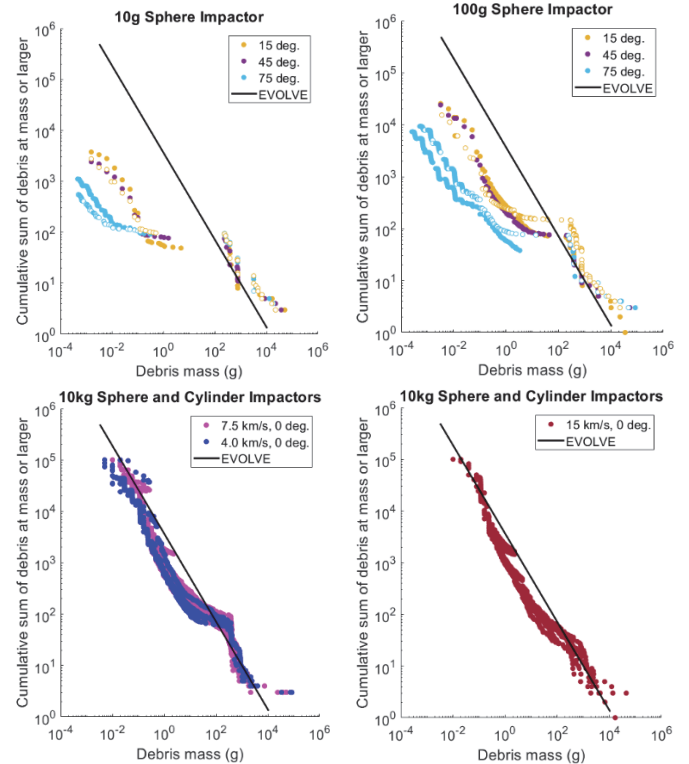


FIGURE 6: CUMULATIVE SUM OF DEBRIS VS. DEBRIS MASS. (TOP) LETHAL NON-TRACKABLE DEBRIS FOR THE 10 g IMPACTOR CASE (LEFT SIDE) AND THE 100 g IMPACTOR CASE (RIGHT SIDE). HOLLOW CIRCLES INDICATE $v = 4$ km/s. (BOTTOM) LARGE CATASTROPHIC IMPACTORS FOR ALL 4 km/s AND 7.5 km/s CASES (LEFT SIDE) AND ALL 15 km/s CASES (RIGHT SIDE), INCLUDING 19 cm, 30 cm, AND 100 cm DIAMETER IMPACTORS.

4. CONCLUSION

In this paper, we have presented a series of numerical hydrocode runs modeling the hypervelocity impact of non-trackable lethal debris and catastrophic large objects on a notional 1 m³ satellite bus. This method allowed us to predict debris creation for sub-catastrophic conditions under the 40 J/g threshold and for novel impactor and target configurations not considered by NASA models. We compared SPHC results to results from NASA’s breakup model and to linear fits with existing experimental data.

For cases at or below the 40 J/g threshold, NASA’s EVOLVE model overpredicted the amount of generated debris by several orders of magnitude compared to hydrocode results. However, hydrocode results and experimental fit data for mass-to-length predictions showed good agreement.

ACKNOWLEDGEMENTS

The authors thank the Institute for Defense Analyses for supporting this work. Our special thanks go to Cameron Liang,

Hannah Yi, Courtney Au-Yeung, Rebeca Rodriguez, Jason Sheldon, and Dan Pechkis for their technical feedback and meaningful collaboration.

[15] Lee, Minhyung, and Stephan J. Bless. "Cavity Models for Solid and Hollow Projectiles." *International Journal of Impact Engineering* 21.10 (1998): 881-894.

REFERENCES

- [1] National Science and Technology Council. "National Orbital Debris Research and Development Plan." January 2021.
- [2] Truitt, A. "IARPA's Space debris Identification and Tracking (SINTRA) Program." *Proceedings of the Advanced Maui Optical and Space Surveillance (AMOS) Technologies Conference*. Maui, Hawaii, September 19-22, 2023.
- [3] Nicholas, Andrew C., et al. "On-Orbit Optical Detection of Lethal Non-trackable Debris." *Acta Astronautica* 212 (2023): 177-186.
- [4] Johnson, Nicholas L., et al. "NASA's New Breakup Model of EVOLVE 4.0." *Advances in Space Research* 28.9 (2001): 1377-1384.
- [5] Cowardin, Heather M., et al. "Optical Characterization of DebrisSat Fragments in Support of Orbital Debris Environmental Models." *The Journal of the Astronautical Sciences* 68 (2021): 1186-1205.
- [6] Murray, James, et al. "Analysis of the DebrisSat Fragments and Comparison to the NASA Standard Satellite Breakup Model." *International Orbital Debris Conference (IOC)*. No. JSC-E-DAA-TN73918. 2019.
- [7] Olivieri, Lorenzo, Cinzia Giacomuzzo, and Alessandro Francesconi. "Analysis of Fragments Larger than 2 mm Generated by a Picosatellite Fragmentation Experiment." *Acta Astronautica* 204 (2023): 418-424.
- [8] Gürgen, S. "A Numerical Study on Hypervelocity Impact Behavior of Metallic Plates." *Mühendis Ve Makina*, 64 No. 712 (2023), 476-491.
- [9] Reynolds, Robert, et al. "NASA Standard Breakup Model, 1998 Revision." LMSMSS-32532. Lockheed Martin Space Operations Company, Bethesda, Maryland, 1998.
- [10] McKnight, D. S., et al. "Satellite Orbital Debris Characterization Impact Test (SOCIT) Series Data Collection Report." Kaman Sciences Corporation, Bloomfield, Connecticut, 1995.
- [11] Krisko, P. H., Matt Horstman, and M. L. Fudge. "SOCIT4 Collisional-Breakup Test Data Analysis: With Shape and Materials Characterization." *Advances in Space Research* 41.7 (2008): 1138-1146.
- [12] Squire, M., et al. "Evaluation of MMOD Risk Predictions with Available On-Orbit Assets." NASA Report NESC-RP-14-01000. NASA, Hampton, Virginia, July 27, 2017.
- [13] Williamsen, J., et al. "Lethal Debris Creation Following Untracked Orbital Debris Impacts on a SmallSat Constellation." *International Orbital Debris Conference*. Sugar Land, Texas, December 4-7, 2023.
- [14] Stellingwerf, R.F. "Smooth Particle Hydrodynamics." *Advances in the Free-Lagrange Method Including Contributions on Adaptive Gridding and the Smooth Particle Hydrodynamics Method*. Vol. 395 (1991): pp. 239-247.

REPORT DOCUMENTATION PAGEForm Approved
OMB No. 0704-0188

The public reporting burden for this collection of information is estimated to average 1 hour per response, including the time for reviewing instructions, searching existing data sources, gathering and maintaining the data needed, and completing and reviewing the collection of information. Send comments regarding this burden estimate or any other aspect of this collection of information, including suggestions for reducing the burden, to Department of Defense, Washington Headquarters Services, Directorate for Information Operations and Reports (0704-0188), 1215 Jefferson Davis Highway, Suite 1204, Arlington, VA 22202-4302. Respondents should be aware that notwithstanding any other provision of law, no person shall be subject to any penalty for failing to comply with a collection of information if it does not display a currently valid OMB control number.

PLEASE DO NOT RETURN YOUR FORM TO THE ABOVE ADDRESS.

1. REPORT DATE (DD-MM-YYYY)		2. REPORT TYPE		3. DATES COVERED (From - To)	
4. TITLE AND SUBTITLE				5a. CONTRACT NUMBER	
				5b. GRANT NUMBER	
				5c. PROGRAM ELEMENT NUMBER	
6. AUTHOR(S)				5d. PROJECT NUMBER	
				5e. TASK NUMBER	
				5f. WORK UNIT NUMBER	
7. PERFORMING ORGANIZATION NAME(S) AND ADDRESS(ES)				8. PERFORMING ORGANIZATION REPORT NUMBER	
9. SPONSORING/MONITORING AGENCY NAME(S) AND ADDRESS(ES)				10. SPONSOR/MONITOR'S ACRONYM(S)	
				11. SPONSOR/MONITOR'S REPORT NUMBER(S)	
12. DISTRIBUTION/AVAILABILITY STATEMENT					
13. SUPPLEMENTARY NOTES					
14. ABSTRACT					
15. SUBJECT TERMS					
16. SECURITY CLASSIFICATION OF:			17. LIMITATION OF ABSTRACT	18. NUMBER OF PAGES	19a. NAME OF RESPONSIBLE PERSON
a. REPORT	b. ABSTRACT	c. THIS PAGE			19b. TELEPHONE NUMBER (Include area code)